# Supplementary Methods

1   Description of the Model

The model describes the phosphorylation and dephosphorylation of the kinases ERK and RSK and their interaction with the viral protein ORF45. The architecture of the model captures the binding and catalytic events correctly where docking motif, docking groove, and catalytic site accessibility are taken into account based on mechanistic studies. It consists of a set of ordinary differential equations (ODEs) and is simulated and analyzed using the Python package "SloppyCell" and custom written scripts in Python. Two main versions of the model are considered, one that describes the SPR experiments and one that describes the *in vitro* and *in cell* experiments. In addition, there is an extended version of the latter that additionally includes two generic RSK substrate species. All models are available in SBML format as supplementary data.

The model consists of the three "basic" molecular species ERK (called `E` in the model), RSK (`R`), and ORF45 (`O`). Each of these species can bind to the other two individually, but one of the species may also be bound to the two others at the same time, thus giving rise to different variants of ternary complexes. The three species can also form a "closed" complex in which each of the species is bound to both of the others.

Apart from engaging in binding reactions, ERK and RSK can also be phosphorylated and dephosphorylated. In the model the phosphorylated forms are abbreviated as `pE` and `pR`, respectively.

Free ERK is phosphorylated by the activated kinase MKK (`pK` in the model) and dephosphorylated by the phosphatase MKP (`P` in the model). RSK is phosphorylated by phosphorylated ERK. Importantly, RSK can be phosphorylated by ERK only when the latter is not bound to ORF45. RSK is dephosphorylated by a phosphatase that is referred to as `P2` in the model. RSK can only interact with the phosphatase when it is not directly bound to ORF45.

The kinase MKK also occurs in an inactive form (`K`). Its activation is guided by upstream processes that are not represented in detail in the model (see Section **??**).
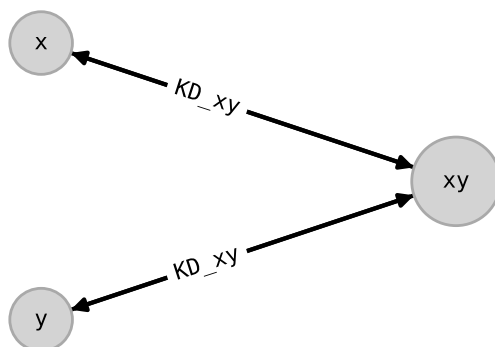
Supplementary Figure 8: Graphical convention.
The reactions occurring in the model are represented using separate arrows from the reactants to the product. Double arrows indicate reversible reactions.

2   Terminology

In order to visualize the model, we use the basic scheme that is illustrated in Supplementary Fig. **??**.

All binding reactions and possible complexes are shown in Supplementary Fig. **??**. At the center of the diagram are the "basic" species (`O`, `R`, `E`, `pE`, and `pR`). Binary complexes are denoted by combining the letters corresponding to the respective basic species (e.g. `EpR` for the binary complex consisting of

ERK and pRSK). For the ternary complexes the names of the species that directly bind are assembled together to groups, and those groups are then concatenated by underscores. So, for example, pEO_pER refers to the ternary complex in which pERK is directly bound to both ORF45 and RSK, but ORF45 and RSK do not directly bind each other.

Aside from the individual molecular species, we introduce variables that represent the total concentration of each of the molecular species and that are referred to as `Otot`, `Rtot`, `Etot`, `pRtot`, and `pEtot`, respectively. They correspond to the sum of concentrations of all species in which the corresponding combination of letters can be found. So, for example, `pRtot` is the sum of the concentrations of all components that are colored either blue or green in the diagram in Supplementary Fig. **??**.
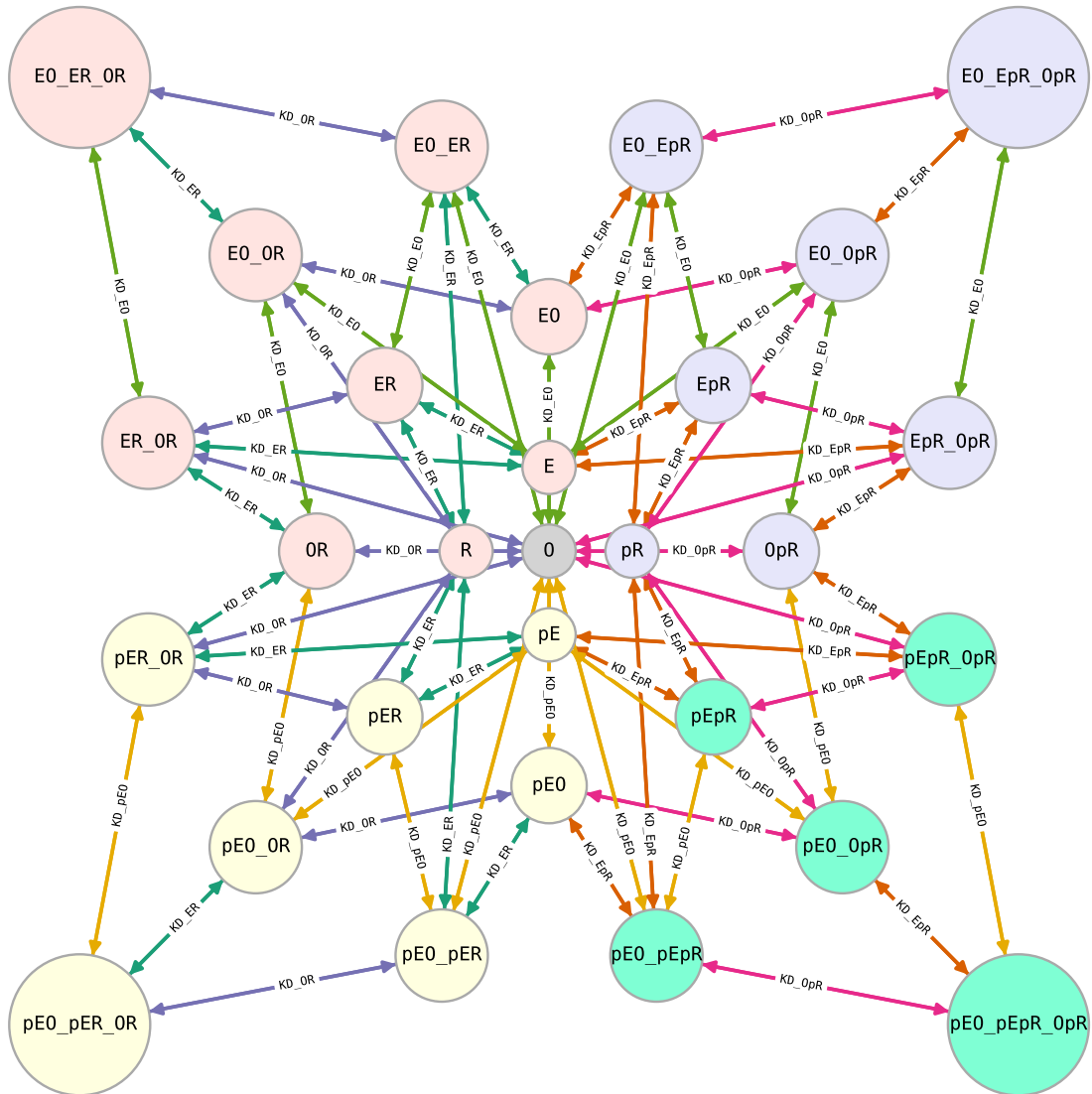
Supplementary Figure 9: Model diagram.
Diagram showing all binding reactions and the possible complexes formed by the three basic components ERK (`E`), RSK (`R`), and ORF45 (`O`). The colors are used to group species that either include the unphosphorylated forms `E` and `R` (red), phosphorylated `pE` and unphosphorylated `r` (yellow), unphosphorylated `E` and phosphorylated `pR` (blue), or both phosphorylated (green). The colors of the arrows serve to highlight reactions with the same dissociation constant.
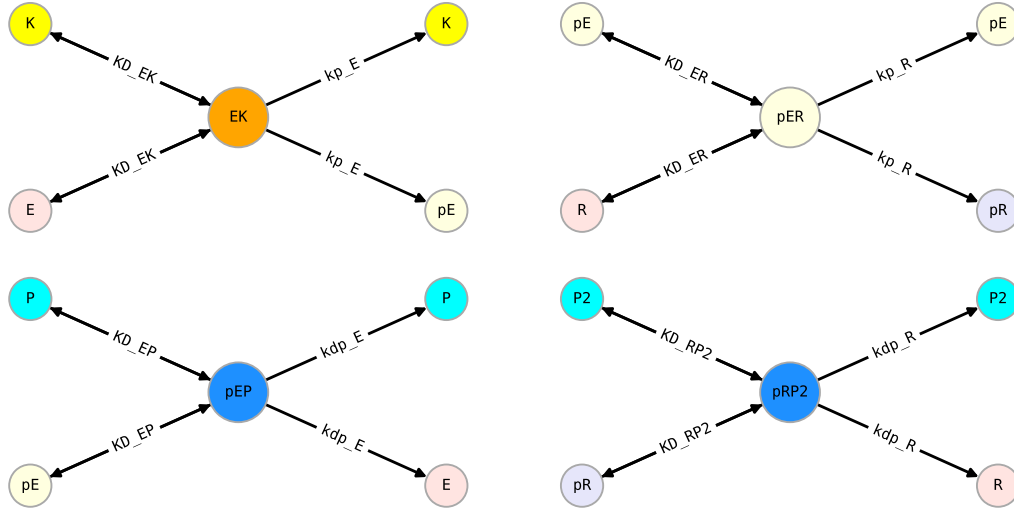
Supplementary Figure 10: Catalytic reactions.
Diagram showing phosphorylation and dephosphorylation in the model. Note that binding reactions are reversible (indicated by double arrows) and catalytic reactions are irreversible. The figure shows only reactions involving the basic species. For the full list of catalytic reactions see section **??**.

3 Model Equations

The full model consists of 34 coupled ODEs. Instead of writing them all down explicitly, we provide the general form of the equations, which is based on straightforward mass-action and Michaelis-Menten kinetics. A full list of all reactions that enter into these equations can be found in Section **??**.

3.1 Association and Dissociation Reactions

All binding and dissociation reactions are reversible and of the form

$$s_i(\mathtt{x}) + s_j(\mathtt{y}) \xrightleftharpoons[\mathtt{koff\_xy}]{\mathtt{kon\_xy}} s_k(\mathtt{xy}), \tag{1}$$
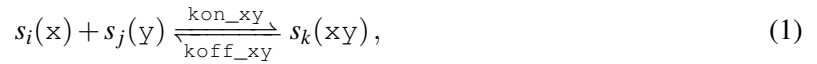
where $s_i(\mathtt{x})$ and $s_j(\mathtt{y})$ refer to the species $\mathtt{x}$ and $\mathtt{y}$ or to complexes containing these species, and $s_k(\mathtt{xy})$ is a complex in which $\mathtt{x}$ and $\mathtt{y}$ are bound. The parameters $\mathtt{kon\_xy}$ and $\mathtt{koff\_xy}$ are the rates of the forward and reverse reactions, respectively. The corresponding differential equation is of the form

$$\frac{d}{dt}[s_k(\mathtt{xy})] = \mathtt{kon\_xy} \cdot [s_i(\mathtt{x})] \cdot [s_j(\mathtt{y})] - \mathtt{koff\_xy} \cdot [s_k(\mathtt{xy})] + \cdots. \tag{2}$$

The square brackets stand for concentrations, and the dots ($\cdots$) indicate that there are possible further reactions that contribute to the formation, transformation or dissociation of the complex $s_k(\mathtt{xy})$. The dissociation constant is defined in the usual way as

$$\mathtt{KD\_xy} = \frac{\mathtt{koff\_xy}}{\mathtt{kon\_xy}}. \tag{3}$$

3.2 Catalytic Reactions

Phosphorylation reactions are of the form

$$\mathtt{k} + \mathtt{s} \xrightleftharpoons[\mathtt{koff\_ks}]{\mathtt{kon\_ks}} \mathtt{ks} \xrightarrow{\mathtt{kp\_s}} \mathtt{k} + \mathtt{p}, \tag{4}$$
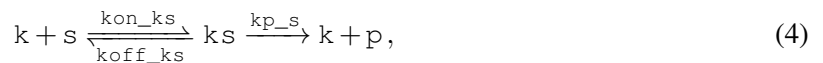
where k is the kinase, s is the substrate (unphosphorlyated form of a species), and p is the product (the phosphorylated form of the same species). The parameter kp_s is the rate of the irreversible catalytic part of the reaction. Dephosphorylation reactions are of analgous form, using the parameter kdp_s for rate of the catalytic step.

The basic scheme of the catalytic reactions is depicted in Supplementary Fig. **??**. Note that kinases and phosphatases bind to their phosphorylated and unphosphorylated substrates with the same rate, but only one of the forms can undergo the catalytic step.

3.3 Activation of the Pathway

For the activation of MKK (the kinase acting upstream of ERK, called K in the model) we use a simplified kinetics of the form
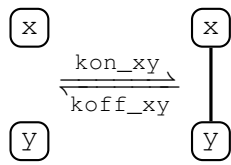
$$\frac{d}{dt}[\text{pK}] = (\text{kp\_K\_bg} + \text{kp\_K\_egf}) \cdot [\text{K}] - \text{kdp\_K} \cdot [\text{pK}], \tag{5}$$

that is, the transition from the the inactive to the active form and its reverse are modeled as single reactions. We distinguish, however, between the activation by the upstream activation of the EGF-pathway (kp_K_egf) and a background activation rate (kp_K_bg) in order to account for the experimental observation that there is a non-zero equilibrium level of pERK already before the stimulation of the pathway.

3.4 The Closed Complex

ERK, RSK, and ORF45 can form a closed ternary complex in which each component is directly bound to the two others. The transition between open ternary complexes and closed complexes has different kinetic properties than the corresponding binary reaction. On the one hand, this is because the conformation of the closed complex may have higher stability leading to a slower dissociation of the binding partners. On the other hand, association occurs between proteins that belong to the same biochemical entity, which makes this reaction different from the usual mass action kinetics. We introduce two parameters, a and d, to account for these differences in the kinetics of association and dissociation, respectively. Supplementary Fig. **??** illustrates this idea schematically.

Formation of binary complex: *Closing of ternary complex:*
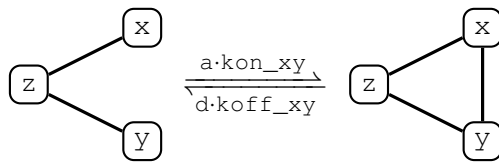
Supplementary Figure 11: Difference in binding kinetics between the formation of a binary complex and the corresponding reaction in the transition from an open to a closed ternary complex. The set of placeholders x, y, and z can be any combination of the basic species (E/pE, R/pR, and O), leading to 8 possibilities of forming a binary and 12 possibilities of closing a ternary complex. While the kon_xy/koff_xy can vary depending on the reaction, the factors a and d are assumed to be the same for all reactions.

The equations that describe the formation of the different closed complexes are of the following form:

$$\frac{d}{dt}[\text{cl}] = \text{a} \cdot \sum_i \text{kon}_i \cdot [\text{op}_i] - \text{d} \cdot \sum_i \text{koff}_i \cdot [\text{cl}]. \tag{6}$$

Here, cl is one of the four closed complexes (corresponding to the four outer vertices in Supplementary Fig. **??**). Each of these closed complexes can be formed from three different open precursors that are

referred to as $\mathtt{op}_i$. The parameters $\mathtt{kon}_i$ and $\mathtt{koff}_i$ are the association and dissocation rates of the corresponding binary reactions. The parameter $\mathtt{d}$ is a dimensionless number that changes each of the binary dissociation rates by the same factor. The parameter $\mathtt{a}$ has a unit of concentration and can be interpreted as the effective concentration that results from bringing the binding partners together in the same complex.

4 Modeling Strategy

We determine plausible ranges for those parameters which were not directly measured by fitting them to different sets of experimental data. We proceed in a step-wise fashion, constraining as many parameters as possible with the simpler SPR and *in vitro* experiments and fitting only the remaining ones to the *in cell* experiments. All parameter values that were used for or obtained from the fitting procedures are listed in Supplementary Table 3.

Because SPR, *in vitro*, and *in cell* experiments are different in many respects, the parameters were not fixed but they were only constrained and were allowed to deviate not much more than by $\pm 10\%$ from the determined value. Note though, that these constraints are not strict, but that deviations add to the overall cost function used for the optimization (For details see the documentation of SloppyCell).

In the main figures we only show the simulations corresponding to the best fit. However, SloppyCell allows for an exhaustive search of the parameter space to generate all parameter sets that are statistically consistent with the data. This is particularly important for so-called "sloppy" models in which many parameters are poorly constrained. As we show, however, the parameters in our model are reasonably well-constrained, and the model predictions still hold even if based on an ensemble fit (Supplementary Fig. 7).

4.1 SPR Experiments

We use the SPR data to obtain the dissociation rates for the binary reactions between ppERK, RSK, and ORF45. In addition, the experiment including all three species allows us to estimate the parameters $\mathtt{a}$ and $\mathtt{d}$ which describe the behavior of the closed ternary complex.

In SPR experiments a protein of interest (the ligand) is stably bound to a surface and can associate with molecules (the analyte) within a solution that flows along the surface. Therefore, the concentration of the free analyte stays constant in the association phase. Thus, for the analytes in our experiments (ppERK and ORF45), we have the following conservation relations:

$$[\mathtt{pE}] = \mathtt{pEtot} - \sum_i [s_i(\mathtt{pE})] = \text{const.} \tag{7}$$

$$[\mathtt{O}] = \mathtt{Otot} - \sum_i [s_i(\mathtt{O})] = \text{const.}, \tag{8}$$

where, as before, the $s_i(\mathtt{E})$, $s_i(\mathtt{pE})$ and $s_i(\mathtt{o})$ denote all the possible complexes that include $\mathtt{E}$ and $\mathtt{O}$, respectively.

For the ligands (RSK and ORF45[1]), by contrast, the total amount is constant, leading to the following conservation relation:

$$\mathtt{Rtot} = [\mathtt{R}] + \sum_i [s_i(\mathtt{R})] = \text{const.} \tag{9}$$

$$\mathtt{Otot} = [\mathtt{O}] + \sum_i [s_i(\mathtt{O})] = \text{const.} \tag{10}$$

Another peculiarity of the SPR experiments is that it measures the mass of the complexes and not their concentrations. In order to compare the simulations to the data from the experiments involving two

---

[1]Note that ORF45 appears both as ligand and as analyte in different experiments.

analytes we therefore need to take into account the relative weight of the different proteins. For this purpose we introduce a new variable

$$\text{Rcomp} = \text{E\_weight} \cdot \sum_i [s_i(\text{ER})] + \text{O\_weight} \cdot \sum_i [s_i(\text{OR})], \qquad (11)$$

where `E_weight` and `O_weight` denote the relative molecular weights of ERK and ORF45, and the $s_i(\text{ER})$ and $s_i(\text{OR})$ denote all the complexes with RSK in which ERK and ORF45 occur, respectively. For all our simulations we chose

$$\text{O\_weight} = 1 \quad \text{and} \quad \text{E\_weight} = 6.3, \qquad (12)$$

in agreement with a molecular weight of 6541Da for ORF45 and 41389Da for ERK2. The absolute weights are not important for the modeling because the data are given in arbitrary units, and we allow for a scaling factor that converts model units into the experimental units. This scaling factor is optimized along with the parameter fit. For the same reason, the absolute amount of ligand bound to the surface does not matter for the modeling results. We choose $\text{Rtot} = 1\mu M$ and $\text{Otot} = 1\mu M$ in the respective experiments.

The model is fit to both the association and the dissociation phase of the experiments. We model the dissociation phase by setting the relevant association rates to zero. All parameters obtained in the fit can be found in Supplementary Table 3.

4.1.1 RSK and ppERK

In this case RSK is the ligand, and ppERK is the analyte. We use a previously measured value of $\text{KD\_ER} = 2.5\mu M$ (see Supplementary Fig. 4b and 5a). We fit the model to two experiments with different analyte concentrations of $[\text{pE}] = 0.12\mu M$ and $[\text{pE}] = 1.11\mu M$.

4.1.2 RSK and ORF45

In this case RSK is the ligand, and ORF45 is the analyte. We use a previously measured value of $\text{KD\_OR} = 0.0012\mu M$ (Supplementary Fig. 4b and 5b). We fit the model to two experiments with two different analyte concentrations of $[\text{O}] = 0.0005\mu M$ and $[\text{O}] = 0.0135\mu M$.

4.1.3 ppERK and ORF45

In this case ORF45 is the ligand, and ppERK is the analyte. We use a previously measured value of $\text{KD\_pEO} = 0.8\mu M$ (see Fig. 2a and Supplementary Fig. 5c). We fit the model to one experiment with $[\text{pE}] = 1.66\mu M$.

4.1.4 RSK, ppERK, and ORF45

We use the experiment with all three species to obtain values for the parameters `a` and `d`, which determine the association and dissociation rates for the closed complex. In this case RSK is the ligand, and we have two analytes, ppERK and ORF45 (see Supplementary Fig. 5d). We use the previously measured values of $\text{KD\_pEO} = 0.8\mu M$ and $\text{KD\_OR} = 0.0012\mu M$, and $\text{KD\_ER} = 2.5\mu M$, as well as the values for `koff_ER`, `koff_OR`, and `koff_pEO` from fitting experiments **??-??**.

We fit the model to two experiments with two different conentrations for ppERK, $[\text{pE}] = 0.12\mu M$ and $[\text{pE}] = 1.11\mu M$. The concentration of ORF45 is in both cases $[\text{O}] = 10\mu M$.

4.2 *in vitro* Experiments

The *in vitro* experiments are used to obtain estimates for the parameters related to phosphorylation and dephosphorylation and to see whether parameters obtained in the SPR experiments are consistent. We

constrain those parameters that were previously determined by measurements or by fitting the SPR experiments and leave the remaining ones free.

Differently from the SPR experiments, all total species amounts are constant throughout the experiments. Therefore, we have conservation relations of the form

$$\texttt{xtot} = [\texttt{x}] + \sum_i [s_i(\texttt{x})] = \text{const.} \qquad (13)$$

for all species x, where xtot denotes the total amount, [x] the concentration of free x, and the $[s_i(\texttt{x})]$ the concentrations of the different possible complexes in which x appears.

In line with the experimental setup, we allow all binding reactions to have reached an equilibrium when the experimental intervention starts. For this purpose, we run the simulation for $t = 1000\,\text{min}$ before making the parameter changes that correspond to the intervention.

Experiment 1: MKK, ERK, RSK, $\pm$ ORF45 In this experiment MKK, (unphosphorylated) ERK, and RSK are mixed together with or without ORF45 (Fig. 5a). The initiation of kinase activity is modeled by setting the parameters kcatkin and kcatrp, which determine the phosphorylation of ERK and RSK, respectively, from zero to a positive value at $t = 1000\,\text{min}$. In line with the experiment, the initial concentrations are:

species	value (μM)
Etot	2.0
pE	0.0
Ktot	0.25
Rtot	2.0
Otot	0.0 or 50.0

Experiment 2: ppERK, MKP, $\pm$RSK, $\pm$ORF45 In this experiment (phosphorylated) ppERK is mixed with MKP in the presence or absence of RSK and ORF45 (Fig. 5c). The initiation of phosphatase activity is modeled by setting the parameter Ptot, corresponding to the total amount of MKP, from zero to $1\mu M$ at $t = 1000\,\text{min}$. In line with the experiment, the initial conditions are:

species	value (μM)
Etot	1.0
pE	1.0
Ptot	$0 \rightarrow 1$
Rtot	0.0 or 1.0
Otot	0.0 or 5.0

The optimal parameters resulting from fitting the *in vitro* experiments can be found in Supplementary Table 3. Fig. 6b of the main text shows a visual comparison of data and model simulations.

4.3 *in cell* Experiments

We assume that the *in cell* and the *in vitro* experiments can be modeled in a similar way. That is, we assume that all species are well-mixed and conserved. Additionally, we now also introduce a phosphatase acting on RSK (called P2), and we include the activation reaction of MKK (K) as described in Equation (??). As in the *in vitro* experiments, we allow the system to find an equilibrium, but then the stimulus is simulated by setting the parameter kp_K_egf from zero to a positive value. The initial concentrations are

species	value (μM)
Ktot	1.2
K	1.2
Etot	0.7
Rtot	2.0
Otot	1.0
Ptot	1.0
P2tot	1.0

The optimal parameters resulting from fitting the *in cell* experiments can be found in Supplementary Table 3. Fig. 6c of the main text shows a visual comparison of data and model simulations.

4.4 Model Predictions and Model with Substrates

The model predictions were obtained by simulating the model in the same way as in **??**, using the optimal *in cell* parameter set, except for the indicated changes (see Fig. 6d).

To simulate the effects of different RSK substrates competing with ORF45 (Fig. 8b), we added two species SUBC and SUBF to the model. SUBC competes with ORF45, meaning that it can only bind to pR if pR is not directly bound to O. SUBF, by contrast, can interact with all complexes containing pR. The interactions of both substrates are guided by the parameters kon_pRSUB, koff_pRSUB, kp_pRSUB, and kdp_pRSUB, which we all set to 1 in our simulations since here we are only interested in qualitative effects. We set the total amounts of the two substrates to a small value (0.01) in order to ensure that the behavior of the rest of the model is not affected (i.e. the substrates are only used as read-outs).

5 Full List of Model Reactions

ERK RSK binding

Reaction	Rate law
$E + R \rightleftharpoons ER$	kon_ER·[E]·[R] − koff_ER·[ER]
$pE + R \rightleftharpoons pER$	kon_ER·[pE]·[R] − koff_ER·[pER]
$EO + R \rightleftharpoons EO\_ER$	kon_ER·[EO]·[R] − koff_ER·[EO_ER]
$E + OR \rightleftharpoons ER\_OR$	kon_ER·[E]·[OR] − koff_ER·[ER_OR]
$pEO + R \rightleftharpoons pEO\_pER$	kon_ER·[pEO]·[R] − koff_ER·[pEO_pER]
$pE + OR \rightleftharpoons pER\_OR$	kon_ER·[pE]·[OR] − koff_ER·[pER_OR]
$EO\_OR \rightleftharpoons EO\_ER\_OR$	a·kon_ER·[EO_OR] − d·koff_ER·[EO_ER_OR]
$pEO\_OR \rightleftharpoons pEO\_pER\_OR$	a·kon_ER·[pEO_OR] − d·koff_ER·[pEO_pER_OR]
$E + RP2 \rightleftharpoons ERP2$	kon_ER·[E]·[RP2] − koff_ER·[ERP2]
$pE + RP2 \rightleftharpoons pERP2$	kon_ER·[pE]·[RP2] − koff_ER·[pERP2]
$EO + RP2 \rightleftharpoons EO\_ERP2$	kon_ER·[EO]·[RP2] − koff_ER·[EO_ERP2]
$pEO + RP2 \rightleftharpoons pEO\_pERP2$	kon_ER·[pEO]·[RP2] − koff_ER·[pEO_pERP2]

ERK ORF binding

Reaction	Rate law
$E + O \rightleftharpoons EO$	kon_EO·[E]·[O] − koff_EO·[EO]
$E + OR \rightleftharpoons EO\_OR$	kon_EO·[E]·[OR] − koff_EO·[EO_OR]
$ER + O \rightleftharpoons EO\_ER$	kon_EO·[ER]·[O] − koff_EO·[EO_ER]
$E + OpR \rightleftharpoons EO\_OpR$	kon_EO·[E]·[OpR] − koff_EO·[EO_OpR]
$EpR + O \rightleftharpoons EO\_EpR$	kon_EO·[EpR]·[O] − koff_EO·[EO_EpR]
$ER\_OR \rightleftharpoons EO\_ER\_OR$	a·kon_EO·[ER_OR] − d·koff_EO·[EO_ER_OR]
$EpR\_OpR \rightleftharpoons EO\_EpR\_OpR$	a·kon_EO·[EpR_OpR] − d·koff_EO·[EO_EpR_OpR]
$ERP2 + O \rightleftharpoons EO\_ERP2$	kon_EO·[ERP2]·[O] − koff_EO·[EO_ERP2]
$EpRP2 + O \rightleftharpoons EO\_EpRP2$	kon_EO·[EpRP2]·[O] − koff_EO·[EO_EpRP2]
$EP + O \rightleftharpoons EPO$	kon_EO·[EP]·[O] − koff_EO·[EPO]
$EP + OR \rightleftharpoons EPO\_OR$	kon_EO·[EP]·[OR] − koff_EO·[EPO_OR]
$EP + OpR \rightleftharpoons EPO\_OpR$	kon_EO·[EP]·[OpR] − koff_EO·[EPO_OpR]
$EpK + O \rightleftharpoons EpKO$	kon_EO·[EpK]·[O] − koff_EO·[EpKO]
$EpK + OR \rightleftharpoons EpKO\_OR$	kon_EO·[EpK]·[OR] − koff_EO·[EpKO_OR]
$EpK + OpR \rightleftharpoons EpKO\_OpR$	kon_EO·[EpK]·[OpR] − koff_EO·[EpKO_OpR]
$EK + O \rightleftharpoons EKO$	kon_EO·[EK]·[O] − koff_EO·[EKO]
$EK + OR \rightleftharpoons EKO\_OR$	kon_EO·[EK]·[OR] − koff_EO·[EKO_OR]
$EK + OpR \rightleftharpoons EKO\_OpR$	kon_EO·[EK]·[OpR] − koff_EO·[EKO_OpR]

ppERK ORF binding

Reaction	Rate law
$pE + O \rightleftharpoons pEO$	kon_EO·[pE]·[O] − koff_pEO·[pEO]
$pE + OR \rightleftharpoons pEO\_OR$	kon_EO·[pE]·[OR] − koff_pEO·[pEO_OR]
$pER + O \rightleftharpoons pEO\_pER$	kon_EO·[pER]·[O] − koff_pEO·[pEO_pER]
$pE + OpR \rightleftharpoons pEO\_OpR$	kon_EO·[pE]·[OpR] − koff_pEO·[pEO_OpR]
$pEpR + O \rightleftharpoons pEO\_pEpR$	kon_EO·[pEpR]·[O] − koff_pEO·[pEO_pEpR]
$pER\_OR \rightleftharpoons pEO\_pER\_OR$	a·kon_EO·[pER_OR] − d·koff_pEO·[pEO_pER_OR]
$pEpR\_OpR \rightleftharpoons pEO\_pEpR\_OpR$	a·kon_EO·[pEpR_OpR] − d·koff_pEO·[pEO_pEpR_OpR]
$pERP2 + O \rightleftharpoons pEO\_pERP2$	kon_EO·[pERP2]·[O] − koff_pEO·[pEO_pERP2]
$pEpRP2 + O \rightleftharpoons pEO\_pEpRP2$	kon_EO·[pEpRP2]·[O] − koff_pEO·[pEO_pEpRP2]
$pEP + O \rightleftharpoons pEPO$	kon_EO·[pEP]·[O] − koff_pEO·[pEPO]
$pEP + OR \rightleftharpoons pEPO\_OR$	kon_EO·[pEP]·[OR] − koff_pEO·[pEPO_OR]
$pEP + OpR \rightleftharpoons pEPO\_OpR$	kon_EO·[pEP]·[OpR] − koff_pEO·[pEPO_OpR]
$pEpK + O \rightleftharpoons pEpKO$	kon_EO·[pEpK]·[O] − koff_pEO·[pEpKO]
$pEpK + OR \rightleftharpoons pEpKO\_OR$	kon_EO·[pEpK]·[OR] − koff_pEO·[pEpKO_OR]
$pEpK + OpR \rightleftharpoons pEpKO\_OpR$	kon_EO·[pEpK]·[OpR] − koff_pEO·[pEpKO_OpR]
$pEK + O \rightleftharpoons pEKO$	kon_EO·[pEK]·[O] − koff_pEO·[pEKO]
$pEK + OR \rightleftharpoons pEKO\_OR$	kon_EO·[pEK]·[OR] − koff_pEO·[pEKO_OR]
$pEK + OpR \rightleftharpoons pEKO\_OpR$	kon_EO·[pEK]·[OpR] − koff_pEO·[pEKO_OpR]

ORF RSK binding

Reaction	Rate law
$O + R \rightleftharpoons OR$	kon_OR·[O]·[R] − koff_OR·[OR]
$EO + R \rightleftharpoons EO\_OR$	kon_OR·[EO]·[R] − koff_OR·[EO_OR]
$O + ER \rightleftharpoons ER\_OR$	kon_OR·[O]·[ER] − koff_OR·[ER_OR]
$pEO + R \rightleftharpoons pEO\_OR$	kon_OR·[pEO]·[R] − koff_OR·[pEO_OR]
$O + pER \rightleftharpoons pER\_OR$	kon_OR·[O]·[pER] − koff_OR·[pER_OR]
$EO\_ER \rightleftharpoons EO\_ER\_OR$	a·kon_OR·[EO_ER] − d·koff_OR·[EO_ER_OR]
$pEO\_pER \rightleftharpoons pEO\_pER\_OR$	a·kon_OR·[pEO_pER] − d·koff_OR·[pEO_pER_OR]
$EPO + R \rightleftharpoons EPO\_OR$	kon_OR·[EPO]·[R] − koff_OR·[EPO_OR]
$pEPO + R \rightleftharpoons pEPO\_OR$	kon_OR·[pEPO]·[R] − koff_OR·[pEPO_OR]
$EpKO + R \rightleftharpoons EpKO\_OR$	kon_OR·[EpKO]·[R] − koff_OR·[EpKO_OR]
$pEpKO + R \rightleftharpoons pEpKO\_OR$	kon_OR·[pEpKO]·[R] − koff_OR·[pEpKO_OR]
$EKO + R \rightleftharpoons EKO\_OR$	kon_OR·[EKO]·[R] − koff_OR·[EKO_OR]
$pEKO + R \rightleftharpoons pEKO\_OR$	kon_OR·[pEKO]·[R] − koff_OR·[pEKO_OR]

ORF pRSK binding

Reaction	Rate law
$O + pR \rightleftharpoons OpR$	kon_OR·[O]·[pR] − koff_OpR·[OpR]
$EO + pR \rightleftharpoons EO\_OpR$	kon_OR·[EO]·[pR] − koff_OpR·[EO_OpR]
$O + EpR \rightleftharpoons EpR\_OpR$	kon_OR·[O]·[EpR] − koff_OpR·[EpR_OpR]
$pEO + pR \rightleftharpoons pEO\_OpR$	kon_OR·[pEO]·[pR] − koff_OpR·[pEO_OpR]
$O + pEpR \rightleftharpoons pEpR\_OpR$	kon_OR·[O]·[pEpR] − koff_OpR·[pEpR_OpR]
$EO\_EpR \rightleftharpoons EO\_EpR\_OpR$	a·kon_OR·[EO_EpR] − d·koff_OpR·[EO_EpR_OpR]
$pEO\_pEpR \rightleftharpoons pEO\_pEpR\_OpR$	a·kon_OR·[pEO_pEpR] − d·koff_OpR·[pEO_pEpR_OpR]
$EPO + pR \rightleftharpoons EPO\_OpR$	kon_OR·[EPO]·[pR] − koff_OpR·[EPO_OpR]
$pEPO + pR \rightleftharpoons pEPO\_OpR$	kon_OR·[pEPO]·[pR] − koff_OpR·[pEPO_OpR]
$EpKO + pR \rightleftharpoons EpKO\_OpR$	kon_OR·[EpKO]·[pR] − koff_OpR·[EpKO_OpR]
$pEpKO + pR \rightleftharpoons pEpKO\_OpR$	kon_OR·[pEpKO]·[pR] − koff_OpR·[pEpKO_OpR]
$EKO + pR \rightleftharpoons EKO\_OpR$	kon_OR·[EKO]·[pR] − koff_OpR·[EKO_OpR]
$pEKO + pR \rightleftharpoons pEKO\_OpR$	kon_OR·[pEKO]·[pR] − koff_OpR·[pEKO_OpR]

ERK MKK binding

Reaction	Rate law
$E + K \rightleftharpoons EK$	kon_EK·[E]·[K] − koff_EK·[EK]
$pE + K \rightleftharpoons pEK$	kon_EK·[pE]·[K] − koff_EK·[pEK]
$E + pK \rightleftharpoons EpK$	kon_EK·[E]·[pK] − koff_EK·[EpK]
$pE + pK \rightleftharpoons pEpK$	kon_EK·[pE]·[pK] − koff_EK·[pEpK]
$EO + pK \rightleftharpoons EpKO$	kon_EK·[EO]·[pK] − koff_EK·[EpKO]
$pEO + pK \rightleftharpoons pEpKO$	kon_EK·[pEO]·[pK] − koff_EK·[pEpKO]
$EO\_OR + pK \rightleftharpoons EpKO\_OR$	kon_EK·[EO_OR]·[pK] − koff_EK·[EpKO_OR]
$pEO\_OR + pK \rightleftharpoons pEpKO\_OR$	kon_EK·[pEO_OR]·[pK] − koff_EK·[pEpKO_OR]
$EO\_OpR + pK \rightleftharpoons EpKO\_OpR$	kon_EK·[EO_OpR]·[pK] − koff_EK·[EpKO_OpR]
$pEO\_OpR + pK \rightleftharpoons pEpKO\_OpR$	kon_EK·[pEO_OpR]·[pK] − koff_EK·[pEpKO_OpR]
$EO + K \rightleftharpoons EKO$	kon_EK·[EO]·[K] − koff_EK·[EKO]
$pEO + K \rightleftharpoons pEKO$	kon_EK·[pEO]·[K] − koff_EK·[pEKO]
$EO\_OR + K \rightleftharpoons EKO\_OR$	kon_EK·[EO_OR]·[K] − koff_EK·[EKO_OR]
$pEO\_OR + K \rightleftharpoons pEKO\_OR$	kon_EK·[pEO_OR]·[K] − koff_EK·[pEKO_OR]
$EO\_OpR + K \rightleftharpoons EKO\_OpR$	kon_EK·[EO_OpR]·[K] − koff_EK·[EKO_OpR]
$pEO\_OpR + K \rightleftharpoons pEKO\_OpR$	kon_EK·[pEO_OpR]·[K] − koff_EK·[pEKO_OpR]

ERK MKP binding

Reaction	Rate law
$E + P \rightleftharpoons EP$	kon_EP·[E]·[P] − koff_EP·[EP]
$pE + P \rightleftharpoons pEP$	kon_EP·[pE]·[P] − koff_EP·[pEP]
$EO + P \rightleftharpoons EPO$	kon_EP·[EO]·[P] − koff_EP·[EPO]
$pEO + P \rightleftharpoons pEPO$	kon_EP·[pEO]·[P] − koff_EP·[pEPO]
$EO\_OR + P \rightleftharpoons EPO\_OR$	kon_EP·[EO_OR]·[P] − koff_EP·[EPO_OR]
$pEO\_OR + P \rightleftharpoons pEPO\_OR$	kon_EP·[pEO_OR]·[P] − koff_EP·[pEPO_OR]
$EO\_OpR + P \rightleftharpoons EPO\_OpR$	kon_EP·[EO_OpR]·[P] − koff_EP·[EPO_OpR]
$pEO\_OpR + P \rightleftharpoons pEPO\_OpR$	kon_EP·[pEO_OpR]·[P] − koff_EP·[pEPO_OpR]

RSK PP2 binding

Reaction	Rate law
$pR + P2 \rightleftharpoons pRP2$	kon_RP2·[pR]·[P2] − koff_RP2·[pRP2]
$R + P2 \rightleftharpoons RP2$	kon_RP2·[R]·[P2] − koff_RP2·[RP2]
$ER + P2 \rightleftharpoons ERP2$	kon_RP2·[ER]·[P2] − koff_RP2·[ERP2]
$pER + P2 \rightleftharpoons pERP2$	kon_RP2·[pER]·[P2] − koff_RP2·[pERP2]
$EO\_ER + P2 \rightleftharpoons EO\_ERP2$	kon_RP2·[EO_ER]·[P2] − koff_RP2·[EO_ERP2]
$pEO\_pER + P2 \rightleftharpoons pEO\_pERP2$	kon_RP2·[pEO_pER]·[P2] − koff_RP2·[pEO_pERP2]
$EpR + P2 \rightleftharpoons EpRP2$	kon_RP2·[EpR]·[P2] − koff_RP2·[EpRP2]
$pEpR + P2 \rightleftharpoons pEpRP2$	kon_RP2·[pEpR]·[P2] − koff_RP2·[pEpRP2]
$EO\_EpR + P2 \rightleftharpoons EO\_EpRP2$	kon_RP2·[EO_EpR]·[P2] − koff_RP2·[EO_EpRP2]
$pEO\_pEpR + P2 \rightleftharpoons pEO\_pEpRP2$	kon_RP2·[pEO_pEpR]·[P2] − koff_RP2·[pEO_pEpRP2]

ERK phosphorylation/dephosphorylation

Reaction	Rate law
$\texttt{EpK} \to \texttt{pE} + \texttt{pK}$	$\texttt{kp\_E} \cdot \texttt{[EpK]}$
$\texttt{pEP} \to \texttt{E} + \texttt{P}$	$\texttt{kdp\_E} \cdot \texttt{[pEP]}$

RSK phosphorylation/dephosphorylation

Reaction	Rate law
$\texttt{pER\_OR} \to \texttt{OpR} + \texttt{pE}$	$\texttt{kp\_R} \cdot \texttt{[pER\_OR]}$
$\texttt{pER} \to \texttt{pR} + \texttt{pE}$	$\texttt{kp\_R} \cdot \texttt{[pER]}$
$\texttt{pRP2} \to \texttt{R} + \texttt{P2}$	$\texttt{kdp\_R} \cdot \texttt{[pRP2]}$
$\texttt{EpRP2} \to \texttt{ER} + \texttt{P2}$	$\texttt{kdp\_R} \cdot \texttt{[EpRP2]}$
$\texttt{pEpRP2} \to \texttt{pER} + \texttt{P2}$	$\texttt{kdp\_R} \cdot \texttt{[pEpRP2]}$
$\texttt{EO\_EpRP2} \to \texttt{EO\_ER} + \texttt{P2}$	$\texttt{kdp\_R} \cdot \texttt{[EO\_EpRP2]}$
$\texttt{pEO\_pEpRP2} \to \texttt{pEO\_ER} + \texttt{P2}$	$\texttt{kdp\_R} \cdot \texttt{[pEO\_pEpRP2]}$

MAPK activation

Reaction	Rate law
$\texttt{K} \rightleftharpoons \texttt{pK}$	$(\texttt{kp\_K\_bg} + \texttt{kp\_K\_egf}) \cdot \texttt{[K]} - \texttt{kdp\_K} \cdot \texttt{[pK]}$

Supplementary References

[1] Gògl, G. *et al.* Dynamic control of RSK complexes by phosphoswitch-based regulation. *FEBS J.* **285**, 46–71 (208).

[2] Ikuta, M. *et al.* Crystal structures of the N-terminal kinase domain of human RSK1 bound to three different ligands: Implications for the design of RSK1 specific inhibitors. *Protein Sci.* **16**, 2626–2635 (2007).

[3] Alexa, A. *et al.* Structural assembly of the signaling competent ERK2-RSK1 heterodimeric protein kinase complex. *Proc. Natl. Acad. Sci. U. S. A.* **112**, 2711–2716 (2015).

[4] Durand, D. *et al.* NADPH oxidase activator p67phox behaves in solution as a multidomain protein with semi-flexible linkers. *J. Struct. Biol.* **169**, 45–53 (2010).